

1 **Structural variants are a major source of gene expression differences in humans and**
2 **often affect multiple nearby genes**

3

4 Alexandra J. Scott^{1,2}, Colby Chiang^{1,2}, Ira M. Hall^{1,2,3,*}

5 ¹ McDonnell Genome Institute, Washington University School of Medicine, St. Louis, MO, USA

6 ² Department of Medicine, Washington University School of Medicine, St. Louis, MO, USA

7 ³ Department of Genetics, Yale University School of Medicine, New Haven, CT, USA

8 * Corresponding author

9 Corresponding email: ira.hall@yale.edu (I.M.H.)

10

11 **Keywords:** Structural variation, eQTLs, gene expression outliers

12

13

14

15

16

17

18

19

20

21

22

23

24

25

26

27 **ABSTRACT**

28 Structural variants (SVs) are an important source of human genome diversity but their functional
29 effects are not well understood. We mapped 61,668 SVs in 613 individuals with deep genome
30 sequencing data from the GTEx project and measured their effects on gene expression. We
31 estimate that common SVs are causal at 2.66% of eQTLs, which is a 10.5-fold enrichment
32 relative to their abundance in the genome and consistent with prior work using smaller sample
33 sizes. Duplications and deletions were the most impactful variant types, whereas the
34 contribution of mobile element insertions was surprisingly small (0.12% of eQTLs, 1.9-fold
35 enriched). Multi-tissue analysis of expression effects revealed that gene-altering SVs show
36 significantly more constitutive effects than other variant types, with 62.09% of coding SV-eQTLs
37 active in all tissues with known eQTL activity compared to 23.08% of coding SNV- and indel-
38 eQTLs, while noncoding SVs, SNVs and indels show broadly similar patterns. We also identified
39 539 rare SVs associated with nearby gene expression outliers. Of these, 62.34% are noncoding
40 SVs that show strong effects on gene expression yet modest enrichment at known regulatory
41 elements, demonstrating that rare noncoding SVs are a major source of gene expression
42 differences but remain difficult to predict from current annotations. Remarkably, both common
43 and rare noncoding SVs often show strong regional effects on the expression of multiple genes:
44 SV-eQTLs affect an average of 1.82 nearby genes compared to 1.09 genes affected by SNV-
45 and indel-eQTLs, and 21.34% of rare expression-altering SVs show strong effects on 2-9
46 different genes. We also observe significant effects on rare gene expression changes extending
47 1 Mb from the SV. This provides a mechanism by which individual noncoding SVs may have
48 strong and/or pleiotropic effects on phenotypic variation and disease.

49

50

51

52

53 **INTRODUCTION**

54 Structural variants (SVs) are a diverse class of genetic variation that include copy number
55 variants (CNVs), mobile element insertions (MEIs) and balanced rearrangements at least 50
56 base pairs (bp) in length. While SVs are relatively rare compared to single-nucleotide variants
57 (SNVs) and small insertion or deletion (indel) variants, their size and diversity mean that SVs
58 can disrupt protein-coding genes and genomic regulatory elements through diverse
59 mechanisms. Furthermore, SVs often have more severe consequences compared to smaller
60 variants and previous studies have found that SVs have an outsized impact on human gene
61 expression compared to their relative abundance in the genome (Chiang et al. 2017; Stranger et
62 al. 2007; Sudmant et al. 2015). SVs have also been implicated in the biology of human diseases
63 such as autism spectrum disorder (Brandler et al. 2018; Sebat et al. 2007; Turner et al. 2017;
64 Weiss et al. 2008) and schizophrenia (International Schizophrenia Consortium 2008; Marshall et
65 al. 2017; McCarthy et al. 2009; Walsh et al. 2008). However, SVs are difficult to detect from
66 short-read DNA sequencing data and are often excluded from complex trait association studies.

67 Advances in high-throughput sequencing technologies that have allowed for widespread
68 use of whole genome sequencing (WGS), combined with advances in scaling SV detection
69 algorithms, mean that comprehensive studies of all forms of genetic variation are now possible
70 for large human cohorts. Recent studies of SV in large, deeply-sequenced human cohorts have
71 found that SVs account for 4.0-11.2% of rare high-impact coding alleles (Abel et al. 2020) and
72 are responsible for 25-29% of rare protein-truncating events per genome (Collins et al. 2020).
73 However, few studies to date have examined the functional effects of SV on gene expression
74 and these studies are limited to relatively small cohort sizes or only a few tissue types with
75 available gene expression data (Chiang et al. 2017; Han et al. 2020; Jakubosky et al. 2020;
76 Sudmant et al. 2015).

77 Here, we use deep WGS data and multi-tissue RNA-seq expression data from 613
78 individuals in the Genotype-Tissue Expression (GTEx) project to comprehensively map SVs and

79 to evaluate their impact on both common and rare gene expression changes in up to 48 tissue
80 types (**Supplemental Table S1**). This study expands on our prior analysis of SV in 147 human
81 samples from the GTEx cohort with RNA-seq expression data from 13 different tissues (Chiang
82 et al. 2017) and is the most comprehensive study of SV-eQTLs to date. The expanded cohort
83 size provides greater power to evaluate the impact and mechanisms of SV-associated gene
84 expression changes, particularly for rare SVs.

85

86 RESULTS

87 Variant calling

88 We mapped SVs in 613 individuals from the GTEx v7 release using LUMPY (Chiang et al. 2015;
89 Layer et al. 2014), svtools (Larson et al. 2019), GenomeSTRiP (Handsaker et al. 2011, 2015)
90 and the Mobile Element Locator Tool (MELT) (Gardner et al. 2017) (see **Methods**). Variant calls
91 were filtered and merged using the same approach as in our previous GTEx study (Chiang et al.
92 2017; Li et al. 2017), resulting in a total of 61,668 “high confidence” SVs that are the basis for all
93 subsequent analyses (**Table 1**). Single nucleotide (SNV) and small insertion deletion (indel)
94 variants were mapped using GATK (McKenna et al. 2010) as part of the official v7 release from
95 the GTEx Consortium.

	Detection method	No. variants	Median size (bp)	# of common variants	eVariants
SNV	GATK	37,087,030	1	9,609,545	178,000
Indel	GATK	3,081,270	3	818,401	16,460
Deletion (DEL)	BP	20,954	1,311	4,385	210
	RD	10,252	2,151	8,166	66
Duplication (DUP)	BP	3,388	2,632	1,090	64
	RD	1,598	6,891	896	233
Multi-allelic CNV (mCNV)	RD	4,365	3,602	3,238	460
Inversion	BP	295	1,054	96	2
Reference mobile element insertion (MEI-del)	BP	2,681	306	2,026	88
Non-reference mobile element insertion (MEI-ins)	BP	13,066	280	4,496	91
Other (BND)	BP	5,069	-	2,010	57
All SVs	-	61,668	-	26,409	1,271
All Variants	-	40,229,968	-	10,454,355	195,731

96 **Table 1. Summary of variant types and eQTL mapping.** SVs were detected based on breakpoint evidence (BP) or
97 read-depth evidence (RD). SNVs and indels were called using the Genome Analysis Toolkit (GATK). Common
98 variants (MAF ≥ 0.01) were used to map cis-eQTLs.

99 **Effects of common SVs**

100 We performed *cis*-eQTL mapping of common variants (MAF ≥ 0.01) using a permutation-based
101 mapping approach with FastQTL (Ongen et al. 2016), limiting comparisons to variants within 1
102 Mb of the transcription start site (TSS) of each gene. We performed eQTL analyses in each of
103 the 48 tissues for which expression data was available for at least 70 individuals (**Supplemental**
104 **Table S1**) and defined an eQTL as an eVariant/eGene pair detected in a given tissue. We
105 performed a “joint” eQTL mapping analysis in which SVs, SNVs and indels were simultaneously
106 queried for eQTL status, allowing for direct comparisons between their properties and
107 identification of a likely causal variant. An SV was the lead marker in 2.66% (7,960/299,187) of
108 eQTLs (**Supplemental Table S2**), although this is likely an underestimate of SV causality due
109 to inferior genotyping accuracy for SVs, which biases eQTL fine-mapping analyses against SVs.
110 While this estimate of the contribution of SVs is relatively small, it represents an 10.5-fold
111 enrichment over the abundance of SVs in the genome. This result is consistent with our prior
112 analysis of the initial 147 individuals from the GTEx cohort (Chiang et al. 2017). In the same 13
113 tissues evaluated in this previous study, the increased sample size used here allowed us to
114 identify 617 genes with SV-eQTLs that were not identified in the smaller study, though 57 genes
115 from the initial study are no longer SV-eQTLs. Interestingly, 71.82% (5,717/7,960) of all SV-
116 eQTLs identified in this study are noncoding (**Supplemental Fig. S1**), meaning the SV does not
117 intersect with any exons of its associated eGene. This figure is even more striking when eQTLs
118 are collapsed across tissues, where 1,907/2,318 (82.27%) of unique eGene/eSV pairs are
119 noncoding. This also suggests that coding SV-eQTLs are more constitutive as more of them are
120 identified in multiple tissues.

121 A novel aspect of this study is that we used MELT to sensitively map mobile element
122 insertion (MEI) variants, including non-reference insertions that were not detected in our prior
123 GTEx studies. It has been proposed that MEIs may have broad effects on gene expression due

124 to their ability to disrupt genes, promote epigenetic gene silencing, and serve as alternate
125 promoters (Payer and Burns 2019; Chuong et al. 2017); however, there has been scant data in
126 humans to address this. We found that only 0.12% (353/299,187) of eQTLs had an MEI as the
127 lead marker. Although this is a 1.9-fold enrichment of predicted causal MEIs relative to their
128 abundance (0.06% of common variants), MEIs were far less likely than other SV types to be the
129 lead marker (e.g., mCNVs are enriched 45-fold, duplications 38-fold and deletions 3.3-fold).
130 Thus, despite compelling molecular evidence for the functional potential of MEIs, our results
131 suggest that they are only slightly enriched as causal eQTL variants relative to SNVs and indels
132 and are depleted relative to other SVs, on average.

133 We found that not only do SVs have larger effect sizes compared to SNPs and indels, as
134 noted in previous studies (**Supplemental Fig. S1**) (Jakubosky et al. 2020; Chiang et al. 2017),
135 they are also more likely to alter the expression of multiple nearby genes. Each eSV affects an
136 average of 1.82 unique eGenes while SNVs and indels affect an average of 1.09 unique
137 eGenes. Although this effect is partially explained by large SVs that alter the copy number of
138 multiple adjacent genes, there is also a significant difference for genes affected by noncoding
139 eVariants: on average, eSVs affect 1.50 unique eGenes for which they do not intersect any
140 exons of the eGene, compared to an average of 1.04 unique eGenes for SNVs and indels
141 ($p=1.02\times10^{-55}$, one-sided Mann-Whitney U test) (**Fig. 1B-D**). These noncoding effects are
142 most pronounced for duplications ($p=6.10\times10^{-53}$) and mCNVs ($p=4.75\times10^{-56}$), which are the only
143 two categories of noncoding SVs that affect significantly more eGenes than point variants. This
144 result indicates that causal SVs are generally more impactful than causal point variants, both in
145 terms of their per-gene effect sizes as well as their potential to affect multiple genes. These
146 results also suggest that SVs are more likely to disrupt key regulatory elements and/or alter
147 higher-order genome architecture, allowing individual variants to affect multiple genes.

148 To investigate the functional mechanisms of expression-altering SVs, we defined a set of
149 putative causal SVs using a score generated by taking the product of the causal probability

150 calculated using CAVIAR (Hormozdiari et al. 2014) and the fraction of heritability attributed to
151 the SV calculated using GCTA (Yang et al. 2011) (**Supplemental Table S3**), as described
152 previously (Chiang et al. 2017). At each eGene we selected the SV within the *cis*-region that
153 had the strongest association with the eGene's expression and allocated these 10,911 unique
154 SVs into six bins on the basis of causality score quantiles, with the least-causal bin containing
155 the 50% of SVs with the lowest scores. Next, we measured the enrichment of SVs in each
156 causality bin at a diverse set of genomic annotations and in the core 15 chromatin segmentation
157 states from the Roadmap Epigenomics Project using a permutation test based on shuffled
158 genomic positions (**Supplemental Fig. S2-S3; see Methods**). SVs in the most causal quantiles
159 were strongly enriched in the exons of their associated eGenes, which is expected and confirms
160 that our causality score is informative. We also observed an enrichment of causal SVs in the 10
161 kb regions upstream of the TSS and downstream of the 3' UTR of the associated eGene.
162 Additionally, there is a small enrichment of the causal SVs in segmental duplications, which is
163 likely driven by large mCNVs at multi-copy genes. However, predicted causal SVs were not
164 enriched in any other genomic features tested, which suggests that while eSVs are generally
165 found relatively close to their eGenes, they may be altering expression through diverse
166 mechanisms and our study is underpowered to identify enrichments in specific regulatory
167 element classes. Alternatively, existing annotations may be insufficiently informative to detect
168 functional enrichments for the variants and tissues analyzed here.

169 The number and diversity of tissues with available expression data allows us to evaluate
170 the tissue specificity of eQTLs. We hypothesized that SVs might have more ubiquitous effects
171 on gene expression than point variants due to constitutively-acting dosage changes or due to
172 complete deletion or duplication of regulatory elements rather than more subtle effects, for
173 example, on transcription factor binding. To allow for facile comparisons between variant types,
174 we limited this analysis to variant-gene pairs with a significant association in our eQTL analysis
175 for which expression data was available across all 48 tissues. We used METASOFT (Han and

176 Eskin 2011) to evaluate eQTL activity across all tissues and limited this analysis to eQTLs for
177 which active ($m>0.9$) or inactive ($m<0.1$) status could be determined in at least 43 tissues. We
178 found that coding SV-eQTLs are more constitutive than other eQTL classes, showing activity
179 across a larger proportion of tissues compared to SNV- and indel-eQTLs (**Fig. 1E**). Whereas
180 92.16% of coding SV-eQTLs are constitutively active – defined here as active in >75% of
181 tissues with known status – only 74.12% of coding SNV- and indel-QTLs are constitutive.
182 However, the result at noncoding eQTLs is less clear: 74.86% of noncoding SV-eQTLs are
183 constitutively active as defined above and 74.12% of noncoding SNV- and indel-eQTLs are
184 constitutive, which suggests that there are not significant differences between these variant
185 categories. However, when we examine noncoding eQTLs that are active in 100% of tissues
186 with known activity, 44.44% of noncoding SV-eQTLs are active in all known tissues compared to
187 26.23% of noncoding SNV- and indel-eQTLs (**Supplemental Fig. S4**). Overall this analysis
188 shows that coding SVs typically impact expression across many tissues, whereas smaller and
189 noncoding variants tend to affect gene expression on a more tissue-specific basis. In contrast to
190 coding SV-eQTLs, noncoding SV-eQTLs show similar patterns of tissue specificity to noncoding
191 SNV- and indel-eQTLs, indicating that these variant types are likely to function through similar
192 mechanisms. However, it is important to note that noncoding SV-eQTL activity could not be
193 determined by METASOFT in many tissues (**Supplemental Fig. S5**), so it is possible that the
194 true tissue specificity of noncoding SVs may differ from noncoding SNVs and indels. This
195 appears to be the result of relatively large effect-size standard errors for SV-eQTLs that result
196 from genotyping inaccuracies. While METASOFT can determine cross-tissue eQTL activity
197 when effect sizes are large despite large standard errors, as seen in coding SV-eQTLs, when
198 effect sizes are small but effect size errors are large, the algorithm often cannot confidently
199 judge activity (**Supplemental Fig. S6**).
200

201 **Effects of rare SVs**

202 Rare SVs are enriched near genes with highly aberrant expression (Chiang et al. 2017) and are
203 more likely to have large effect sizes compared to other variant types (Li et al. 2017). To assess
204 the effects of rare SVs on gene expression, we identified genes in which individuals displayed
205 highly aberrant gene expression levels compared to the dataset as a whole. We limited this
206 analysis to the 513 individuals of European descent to reduce the effects of population
207 stratification and limited our analyses to the 47 tissues in which data were available for at least
208 70 European individuals (**Supplemental Table S1**). We defined 26,289 autosomal multi-tissue
209 gene expression outliers (median $|Z| \geq 2$ across all tissues in an individual) and 173,061
210 autosomal “tissue-restricted” outliers with highly aberrant expression ($|Z| \geq 4$) in two or more
211 tissues in the same individual. Next, we identified 13,768 “singleton” SVs no larger than 1 Mb in
212 size that were positively genotyped in one individual. These rare SVs are strongly enriched
213 within the gene body and flanking sequence of multi-tissue gene expression outliers compared
214 to the null expectation in 1,000 random permutations of the outlier sample names, with
215 enrichment decreasing as flanking distance increases (**Supplemental Fig. S7**). The enrichment
216 of rare SVs in close proximity (14.1-fold enriched within 5 kb; 95% confidence interval (CI), 8.7-
217 25.1; $p < 0.001$) to multi-tissue gene expression outliers is consistent with our prior work (Chiang
218 et al. 2017), but the increased power in this study allows us to observe enrichment at greater
219 distances as well. At flanking distances as large as 50 kb we observe a 6.4-fold enrichment
220 (95% CI 4.9-8.8; $p < 0.001$) of rare SVs around multi-tissue outliers, suggesting that rare SVs
221 contribute to rare expression differences even from relatively large genomic distances.
222 Importantly, because gene expression values can only decrease to 0, a conservative Z-score
223 limit such as the one used for tissue-restricted outliers favors gene expression outliers with
224 increased expression, thus limiting our ability to detect SVs associated with decreased
225 expression (**Supplemental Fig. S8**). However, these conservative outlier definitions, combined
226 with the above enrichment results, provide confidence in the set of outlier-associated SVs.

227 A total of 539 unique outlier-associated SVs are located in the gene body and 50 kb
228 flanking region of gene expression outliers (**Fig. 2A; Supplemental Table S4**). Notably, 62.34%
229 (336/539) of these are noncoding SVs that do not affect the coding sequence of one or more
230 expression outliers. This contradicts the general assumption that rare SVs typically act through
231 gene dosage effects. In total, 16.92% (31,978/188,988) of expression outliers are associated
232 with a rare SV, although outliers can also arise via non-genetic mechanisms. To evaluate the
233 relative potential of different SV types or sizes to cause expression outliers, we calculated the
234 odds ratio (OR) of being outlier-associated for the SV category of interest compared to all other
235 SVs. Duplications (OR 4.07) and mCNVs (OR 1.87) are most likely to be associated with an
236 expression outlier, MEIs are least likely (OR 0.25) (**Fig. 2B**) and larger SVs are more likely to be
237 outlier-associated regardless of type (**Fig. 2C**). However, many outlier-associated SVs are
238 smaller in size (**Fig. 2D**). For example, 13.33% (50/375) of SVs associated with tissue-restricted
239 outliers are smaller than 1 kb and nearly half (49.33%; 185/375) are smaller than 10 kb. Multi-
240 tissue outlier-associated SVs tend to be slightly larger, with only 4.98% (12/241) smaller than 1
241 kb and 35.27% (85/241) smaller than 10 kb. Overall these results provide further evidence that
242 rare SVs often affect gene expression through more complex mechanisms than large, dosage-
243 altering events.

244 We next sought to determine if rare outlier-associated SVs are enriched in annotated
245 genomic features. Although there was little signal in our enrichment analysis of common SVs,
246 as described above, rare variants typically have larger effect sizes and are more likely to be
247 deleterious. For this analysis, we defined a set of “control” SVs that are located within or near
248 genes but do not exhibit expression effects. We identified 1,405 singleton SVs (1,327
249 noncoding) located within 50 kb of autosomal genes that showed consistent expression levels
250 ($|Z| < 1$) across all tissues in an individual. Although this is not an ideal set of control SVs
251 considering that some may in fact alter gene expression in tissues or developmental timepoints
252 for which expression was not measured, it is nonetheless a relatively conservative set of likely-

253 nonfunctional SVs that can be used for comparison to outlier-associated SVs. We examined the
254 overlap of both outlier- and control-associated noncoding SVs with annotated genomic features
255 and with segmentation states from the Roadmap Epigenomics Project core 15-state model (**Fig.**
256 **3A**). We observed significant enrichment of outlier-associated SVs in 5 of the 34 evaluated
257 features and chromatin states (Fisher's Exact test; Bonferonni $p < 0.05$). Most of these
258 significant associations are in Roadmap Epigenomics Project segmentation states in close
259 proximity to transcribed genes, including transcription at the 5' and 3' end of genes showing
260 both promoter and enhancer signatures, active transcription start sites and regions flanking
261 active transcription start sites. We also observed significant enrichment in the Roadmap
262 Epigenomics Project segmentation state associated with zinc finger protein genes and in
263 enhancer annotations from Genehancer. It is important to note, however, that the number of
264 overlaps observed in this analysis is small and increased power might change these results.
265 Thus, while rare SVs appear to have dramatic effects on gene expression, most existing
266 functional annotations are not very informative. Consistent with this, the distribution of SV
267 impact scores (Ganel et al. 2017) is not significantly different between expression-altering SVs
268 and control SVs (**Supplemental Fig. S9**).

269 Interestingly, we found that 115 (21.34%) outlier-associated SVs are associated with
270 more than one expression outlier and that 8 (1.48%) are associated with 5-9 expression outliers,
271 suggesting that many rare SVs may have regional effects. In order to evaluate these broader
272 regional effects of rare expression-altering SVs, we relaxed the definition for aberrant
273 expression to generate a set of "secondary" expression outliers in which the tissue-restricted
274 ("primary") outlier absolute Z-score cutoff was reduced to 3 in at least two tissues. We found
275 significantly more primary and secondary outliers within 1 Mb of the 469 tissue-restricted outlier-
276 associated SVs compared to the 1,496 control-associated SVs and to a null distribution in which
277 we randomly shuffled the sample names of outlier-associated SVs 1,000 times and calculated
278 the median number of associated outlier genes (**Fig. 3B,C**). This increase is especially

279 pronounced for secondary outliers whose coding regions do not overlap with the associated SV.
280 We observe that noncoding outlier-associated SVs are associated with an average of 1.44
281 primary outliers ($|Z| \geq 4$) compared to an average of 0.02 associated primary outliers surrounding
282 the shuffled null SVs ($p\text{-value} = 2.78 \times 10^{-106}$; one-sided Mann-Whitney U test). These differences
283 remain for secondary outliers, with an average of 3.34 secondary outliers found in the expanded
284 region surrounding noncoding outlier-associated SVs compared to an average of 0.54
285 secondary outliers for the shuffled null ($p\text{-value} = 4.94 \times 10^{-76}$; one-sided Mann-Whitney U test).
286 These results suggest that rare SVs have far-reaching effects on gene expression and that
287 these effects are primarily driven by noncoding regulatory mechanisms rather than changes to
288 gene copy number.

289

290 **DISCUSSION**

291 We have comprehensively mapped SVs from WGS data in 613 individuals from the GTEx
292 dataset and analyzed the impact of both common and rare SV on human gene expression. Our
293 findings confirm results from previous analyses that SVs make an outsized contribution to
294 common gene expression changes compared to their abundance in the genome and play an
295 important role in rare gene expression differences (Chiang et al. 2017). A novel aspect of this
296 study is the inclusion of a comprehensive set of MEI insertions, including those present in the
297 GTEx samples but not the reference genome. We observed that MEIs do not play an especially
298 important role in determining gene expression differences. In contrast, we found that mCNVs
299 play an extremely impactful role, being 45-fold enriched among eQTL lead markers compared to
300 their abundance in the genome and more likely to be associated with gene expression outliers
301 ($OR = 1.88$). mCNVs were found to give rise to most human variation in gene dosage
302 (Handsaker et al. 2015), but our findings indicate that noncoding functional mCNVs are also
303 abundant in the human genome.

304 One of the major motivators for studies such as this one is to understand the role of
305 genetic variation in affecting gene transcription. Unfortunately, expression-altering SVs were not
306 well correlated with any specific functional annotations other than proximity to genes, and thus
307 existing annotations are unlikely to be informative for modeling functional variant effects. This
308 may simply be due to a lack of power given that SVs are such a diverse class of variants that
309 can affect large genomic segments and have the potential to affect gene expression through
310 diverse mechanisms, and our sample size is limited to 11,026 common SVs and 539 rare SVs
311 predicted to be functional. Alternatively, the annotations currently available may be inadequate.

312 Nonetheless, it is clear that SVs have broad regional impacts on human gene
313 expression, with individual variants frequently affecting multiple genes. Interestingly, these
314 effects are not driven by large CNVs that alter the dosage of multiple coding sequences, as one
315 might naively expect, but are most commonly observed for noncoding variants: common
316 noncoding eSVs affect an average of 1.50 unique genes and rare noncoding SVs are
317 associated with an average of 1.44 primary expression outlier genes. This observation suggests
318 a mechanism by which rare noncoding SVs may be especially deleterious, and may help
319 explain why prior work has estimated that a surprisingly large number of rare noncoding
320 deletions – an average of 19.1 per individual – appear to be under strong purifying selection
321 (Abel et al. 2020). Furthermore, the burden of *de novo* CNVs has been associated with autism
322 spectrum disorder, including for noncoding variants (Turner et al. 2017; Turner and Eichler
323 2019). Our results provide a mechanism through which individual noncoding SVs can have
324 strong and potentially pleiotropic effects, and thus a higher potential to contribute to disease.

325 While this study represents the most comprehensive analysis of the impact of SVs on
326 human gene expression to date, our callset is missing some of the most repetitive classes of
327 SV, such as short tandem repeats. As long read sequencing and variant calling methods
328 improve, we will be able to gain additional insights into repetitive variants in the most complex
329 regions of the genome. Despite the limitations of short-read sequencing data, this study

330 demonstrates the importance of comprehensive variant detection when evaluating genomic
331 variants that contribute to gene expression and disease. SVs have a disproportionately large
332 effect on common and rare gene expression changes and often affect multiple genes. Our
333 findings reinforce the importance of comprehensive variant detection in the design of future trait
334 mapping studies.

335

336 **METHODS**

337 **Call set generation**

338 We obtained 613 whole-genome sequencing BAM files from the GTEx v7 release (dbGap
339 accession phs000424.v7.p2, accessed 1 June 2016). Structural variant calls were generated
340 using both the SpeedSeq v0.1.1 pipeline (Chiang et al. 2015), which performs sample-level
341 breakpoint detection via LUMPY v.0.2.13 (Layer et al. 2014) followed by population-scale
342 merging and genotyping of SV calls via svtools v0.3.1 (Larson et al. 2019) and the
343 GenomeSTRiP v2.00.1636 read-depth analysis pipeline (Handsaker et al. 2011), as described
344 in our preliminary GTEx study (Chiang et al. 2017). GenomeSTRiP false discovery rate (FDR)
345 was evaluated based on available Illumina Human Omni 5M gene expression array data
346 (n=161) using the GenomeSTRiP IntensityRankSumAnnotator. We limited GSCNQUAL to ≥ 1
347 for GenomeSTRiP deletions and to ≥ 8 for multiallelic copy number variants, corresponding to an
348 FDR of 10%. The GSCNQUAL cutoff for GenomeSTRiP duplications was set at ≥ 17 , the point
349 at which the FDR plateaued at 15.1% and did not fluctuate more than $\pm 1\%$ for over 50 steps of
350 increasing GSCNQUAL score. Redundant Lumpy and GenomeSTRiP calls were merged as
351 previously described (Chiang et al. 2017). Additionally, we ran the Mobile Element Locator Tool
352 (MELT) v2.1.4 using MELT-SPLIT to identify ALU, SVA and LINE1 insertions into the test
353 genomes (Gardner et al. 2017). We retained MELT calls categorized as “PASS” in the VCF info
354 field that had an ASSESS score ≥ 3 and SR count ≥ 3 . Genome Analysis Toolkit (GATK)
355 HaplotypeCaller v3.4 (McKenna et al. 2010) SNV and indel calls were obtained from the GTEx

356 consortium (dbGap accession phs000424.v7.p2, accessed 1 June 2016). We use allele balance
357 instead of genotype for analyses described in this paper because it is tolerant to alignment
358 inefficiencies for the alternate SV allele. For MEIs identified by MELT, we converted generated
359 genotypes (0/0, 0/1, 1/1) to integer values (0, 1, 2) that were used as a proxy for allele balance
360 to allow for comparable analyses on these variants.

361

362 **Common eQTL mapping**

363 We mapped *cis*-eQTLs in each of the 48 tissues for which both WGS data and RNA-seq data
364 was available in ≥ 70 individuals. Available tissues and those used in each analysis are listed in
365 **Supplemental Table S1**. We refer to EBV-transformed lymphocytes and transformed
366 fibroblasts as tissue types throughout this study for convenience. Biospecimen collection, RNA-
367 seq data alignment, RPKM calculations and data normalization were previously described
368 (Lappalainen et al. 2013; Chiang et al. 2017).

369 We selected common genetic markers, defined as having MAF ≥ 0.01 , for eQTL
370 mapping. We performed a joint *cis*-eQTL analysis that included 26,409 common SVs, as well as
371 9,609,545 common SNVs and 818,401 common indels detected using GATK, to allow for a fair
372 comparison of the contribution of different variant types. We used FastQTL v2.184 (Ongen et al.
373 2016) to perform *cis*-eQTL mapping, customized to accomidate the unique architecture of SVs
374 (Chiang et al. 2017), using a *cis* window of 1 Mb on either side of the TSSs of autosomal and X-
375 chromosome genes with a permutation analysis to identify the most significant marker for each
376 gene. For each tissue we applied the same covariates described in Chiang et al. 2017. We
377 corrected for multiple-testing at the gene-level using the Benjamini-Hochberg method with a
378 10% FDR.

379

380 **Feature enrichment**

381 To evaluate whether SVs that cause common gene expression changes are enriched in
382 particular genomic features, we calculated a previously described causality score (Chiang et al.
383 2017) generated by taking the product of the SV heritability fraction obtained from GCTA (Yang
384 et al. 2011) and the causal probability generated by CAVIAR (Hormozdiari et al. 2016) for the
385 strongest-associated SV within the *cis* region of each eQTL. No associated SVs were identified
386 in 199 eQTLs due to the subset of samples with available data in the relavent tissue and thus
387 were not included in enrichment analyses. GCTA heritability estimates could not be calculated
388 for a small number of eQTLs (6,146/299,187) due to nonpositive definite matrices, likely
389 resulting from small sample sizes, and these loci were excluded from feature enrichment
390 analyses. For SVs that were associated with multiple eQTLs or the same eQTL in multiple
391 tissues, we selected the eQTL (tissue/gene pair) for which the SV had the highest causality
392 score. SVs were allocated into bins based on causality score quantiles, with the first bin
393 consisting of SVs in the bottom 50% of causality scores and the other five consisting of deciles
394 of the top 50% of scores.

395 Next, we counted the number of SVs in each bin that intersected with various genomic
396 annotations. We allowed 1 kb of flanking distance surrounding all annotations with the following
397 exceptions: GENCODE exons, no flanking distance; proximity to TSS and 3' gene end, 10 kb of
398 directional flanking distance; topologically associated domain boundaries, 5 kb of flaking
399 distance; Roadmap Epigenomics segmentation states, no flanking distance. SVs associated
400 with multiple eGenes were considered to touch an eGene if they overlapped with the exons of
401 any associated gene. SVs that touched an exon of an associated eGene were excluded from all
402 feature enrichment analyses except for the enrichment of affected eGenes. To generate a
403 shuffled null for comparison, SVs within each causality bin were shuffled with BEDTools v2.23.0
404 (Quinlan and Hall 2010) into non-gapped regions of the genome within 1 Mb of the TSS of a
405 gene. We did not allow shuffled SVs to intersect any exons of their new eGene. We calculated
406 the fold enrichment of the number of SVs that intersect with each genomic feature compared to

407 the median number of intersections observed for 100 randomly shuffled sets within each
408 causality bin. These shuffled sets were also used to empirically derive the 95% confidence
409 intervals.

410 Regions 10 kb upstream of TSS and downstream of 3' gene end were defined based on

411 GENCODE v19 gene positions. DNase hypersensitive regions and enhancer regions with a
412 minimum support of 2 were obtained from the Dragon ENhancers database (DENdb) (Ashoor et
413 al. 2015). We downloaded FunSeq 2.1.0 (Fu et al. 2014) regions and topologically associated
414 domain boundaries from human embryonic stem cells from author websites

415 (http://archive.gersteinlab.org/funseq2.1.0_data/ and

416 http://compbio.med.harvard.edu/modencode/webpage/hic/hESC_domains_hg19.bed).

417 GeneHancer (Fishilevich et al. 2017) enhancer regions for b38 were downloaded from the
418 UCSC genome browser (Kent et al. 2002) and lifted over to b37 using CrossMap v0.2.6 (Zhao
419 et al. 2014). Regions defined by the ENCODE (Encode Project Consortium 2012) project were
420 downloaded from the UCSC genome browser. To evaluate the intersection with the chromatin
421 segmentation state annotations from the Roadmap Epigenomics Project (Kundaje et al. 2015),
422 we downloaded the core 15-state model annotations for all 127 available epigenomes
423 (https://egg2.wustl.edu/roadmap/data/byFileType/chromhmmSegmentations/ChmmModels/core_Marks/jointModel/final). We used BEDTools multiIntersectBed (Quinlan and Hall 2010) to
425 identify genomic intervals where each of the 15 annotations is found in at least 10 of the 127
426 available epigenomes and used these collapsed regions as the annotation intervals for SV
427 intersections.

428

429 **eQTL tissue specificity**

430 We selected significant gene-variant pairs identified in eQTL mapping with available expression
431 data available across all 48 tissues in which eQTL analyses were performed. These pairs were
432 only required to have a significant eQTL in one tissue. We used METASOFT v2.0.0 (Han and

433 Eskin 2011) to perform a meta-analysis of the selected eQTL effect sizes and their standard
434 errors across all 48 tissues. METASOFT employs a mixed effects model (RE2) to generate a
435 posterior probability that an effect exists in each tissue (*m*-value) (Han and Eskin 2012). To
436 allow computational feasibility with the relatively large number of tissues sampled, the Markov
437 Chain Monte Carlo (MCMC) method was used to approximate these values. The *m*-values
438 generated indicate whether a tested eQTL is active ($m>0.9$), inactive ($m<0.1$), or has ambiguous
439 activity ($0.1\leq m\leq 0.9$). Only eQTLs with at least 43 tissues having known (active or inactive)
440 activity were included in analyses. eQTLs with active status in at least 75% of tissues with
441 known activity were defined as “constitutively active.”

442

443 **Identification of expression outliers**

444 We limited outlier analyses to the 513 European individuals, the largest subpopulation in the
445 cohort, who had available WGS data. We performed Z transformation of PEER-corrected
446 expression values without quantile normalization across the 47 tissues for which RNA-seq data
447 was available from the GTEx consortium for at least 70 European individuals (**Supplemental**
448 **Table S1**). We defined two sets of gene expression outliers (gene/sample pairs) among these
449 individuals: “multi-tissue” expression outliers in which an individual’s absolute median Z-score of
450 a gene’s expression across all available tissues was ≥ 2 , as previously described in (Chiang et
451 al. 2017), and “tissue-restricted” outliers in which an individual’s absolute Z score for a gene’s
452 expression was ≥ 4 in at least two different tissues. The two tissue requirement was necessary
453 to eliminate false positive expression outliers resulting from individual tissues with systematically
454 aberrant gene expression profiles for an individual. Additionally, we defined a set of control
455 gene/sample pairs in which an individual’s absolute Z score of a gene’s expression was less
456 than 1 across all tissues for which RNA-seq data was available. For all definitions we limited to
457 gene/sample pairs with data available in at least 5 tissues. We removed one individual (GTEX-
458 14753) from this analysis due an excessive number of expression outliers.

459 **Rare variant association with expression outliers**

460 We identified 15,016 structural variants that were positively genotyped in no more than one
461 individual in the European cohort. Because large rare structural variants tend to affect gene
462 expression through dosage changes, we removed 12 variants larger than 1 Mb in size from this
463 analysis. We calculated the enrichment of singleton SVs overlapping with multi-tissue outlier
464 transcripts and the flanking 5 kb sequence by randomly shuffling the outlier individual names
465 1,000 times to determine the median number of times a rare variant randomly co-occurred with
466 an outlier, as described in (Chiang et al. 2017). We also performed the reciprocal analysis
467 counting the number of outliers that co-occurred within 5 kb of a rare SV. We repeated these
468 calculations for increased outlier-flanking regions of 10 kb, 25 kb, 50 kb and 100 kb. We
469 calculated the odds ratio of being outlier-associated by dividing the ratio of outlier-associated
470 SVs to non-outlier associated SVs in a category of interest (SV type or size) by the ratio of
471 outlier-associated SVs to non-outlier associated SVs for all SVs not included in the category.

472

473 **Feature enrichment for outlier-associated SVs**

474 We performed intersections between the 369 noncoding outlier-associated SVs and the same
475 genomic features and chromatin segmentation states evaluated for eSVs. The above
476 intersections were repeated for the 1,416 noncoding control-associated SVs. We calculated the
477 fold enrichment of outlier-associated SVs in each feature compared to control-associated SVs
478 and determined significant enrichments using a Fisher's Exact Test with Bonferroni correction
479 for multiple testing.

480

481 **Regional effect of rare SVs**

482 To evaluate the broader regional effects of rare, gene expression-altering SVs, we counted the
483 number of tissue-restricted outlier genes, referred to as "primary" outliers, located in the
484 spanning region and 1 Mb of flanking sequence both upstream and downstream of the 469 SVs

485 previously identified as being associated with an expression outlier. We repeated this analysis
486 with a relaxed definition of tissue-restricted expression outliers, referred to as “secondary”
487 outliers, in which the absolute Z score cutoff was reduced from $|Z| \geq 4$ to $|Z| \geq 3$. We compared the
488 number of primary and secondary outliers found in the expanded region surrounding outlier-
489 associated SVs to the expanded region surrounding the 1,224 control-associated SVs. Finally,
490 because the controls defined above do not represent a null expectation, we performed 1,000
491 random permutations of the outlier-associated SV sample names and calculated the median
492 number of associated primary and secondary outliers for each SV in order to determine how
493 frequently rare expression-altering SVs co-occurred with primary and secondary outliers in
494 random individuals.

495

496 **DATA ACCESS**

497 The SV genotype data generated in this study have been submitted to AnVIL
498 (https://app.terra.bio/#workspaces/anvil-datastorage/AnVIL_GTEEx_V7_hg19) under dbGaP
499 accession number phs000424.

500

501 **COMPETING INTEREST STATEMENT**

502 The authors declare no competing interests.

503

504 **ACKNOWLEDGMENTS**

505 The authors thank E.J. Gardner for advice on MELT and R.E. Handsaker for advice on Genome
506 STRiP. This work was supported by a Mr. and Mrs. Spencer T. Olin Fellowship for Women in
507 Graduate Study (A.J.S.) and by the NIH/NHGRI UM1 HG008853 (I.M.H.).

REFERENCES

Abel HJ, Larson DE, Regier AA, Chiang C, Das I, Kanchi KL, Layer RM, Neale BM, Salerno WJ, Reeves C, et al. 2020. Mapping and characterization of structural variation in 17,795 human genomes. *Nature* **583**: 83–89.

Ashoor H, Kleftogiannis D, Radovanovic A, Bajic VB. 2015. DENdb: database of integrated human enhancers. *Database* **2015**. <http://dx.doi.org/10.1093/database/bav085>.

Brandler WM, Antaki D, Gujral M, Kleiber ML, Whitney J, Maile MS, Hong O, Chapman TR, Tan S, Tandon P, et al. 2018. Paternally inherited cis-regulatory structural variants are associated with autism. *Science* **360**: 327–331.

Chiang C, Layer RM, Faust GG, Lindberg MR, Rose DB, Garrison EP, Marth GT, Quinlan AR, Hall IM. 2015. SpeedSeq: ultra-fast personal genome analysis and interpretation. *Nat Methods* **12**: 966–968.

Chiang C, Scott AJ, Davis JR, Tsang EK, Li X, Kim Y, Hadzic T, Damani FN, Ganel L, GTEx Consortium, et al. 2017. The impact of structural variation on human gene expression. *Nature Genetics* **49**: 692–699.

Chuong EB, Elde NC, Feschotte C. 2017. Regulatory activities of transposable elements: from conflicts to benefits. *Nat Rev Genet* **18**: 71–86.

Collins RL, Brand H, Karczewski KJ, Zhao X, Alföldi J, Francioli LC, Khera AV, Lowther C, Gauthier LD, Wang H, et al. 2020. A structural variation reference for medical and population genetics. *Nature* **581**: 444–451.

Encode Project Consortium. 2012. An integrated encyclopedia of DNA elements in the human genome. *Nature* **489**: 57–74.

Fishilevich S, Nudel R, Rappaport N, Hadar R, Plaschkes I, Iny Stein T, Rosen N, Kohn A, Twik M, Safran M, et al. 2017. GeneHancer: genome-wide integration of enhancers and target genes in GeneCards. *Database* **2017**. <http://dx.doi.org/10.1093/database/bax028>.

Fu Y, Liu Z, Lou S, Bedford J, Mu XJ, Yip KY, Khurana E, Gerstein M. 2014. FunSeq2: a framework for prioritizing noncoding regulatory variants in cancer. *Genome Biol* **15**: 480.

Ganel L, Abel HJ, FinMetSeq Consortium, Hall IM. 2017. SVScore: an impact prediction tool for structural variation. *Bioinformatics* **33**: 1083–1085.

Gardner EJ, Lam VK, Harris DN, Chuang NT, Scott EC, Pittard WS, Mills RE, Genomes Project, Consortium, Devine SE. 2017. The Mobile Element Locator Tool (MELT): population-scale mobile element discovery and biology. *Genome Res* **27**: 1916–1929.

Han B, Eskin E. 2012. Interpreting meta-analyses of genome-wide association studies. *PLoS Genet* **8**: e1002555.

Han B, Eskin E. 2011. Random-effects model aimed at discovering associations in meta-analysis of genome-wide association studies. *Am J Hum Genet* **88**: 586–598.

Handsaker RE, Korn JM, Nemesh J, McCarroll SA. 2011. Discovery and genotyping of genome structural polymorphism by sequencing on a population scale. *Nat Genet* **43**: 269–276.

Handsaker RE, Van Doren V, Berman JR, Genovese G, Kashin S, Boettger LM, McCarroll SA. 2015. Large multiallelic copy number variations in humans. *Nat Genet* **47**: 296–303.

Han L, CommonMind Consortium, Zhao X, Benton ML, Perumal T, Collins RL, Hoffman GE, Johnson JS, Sloofman L, Wang HZ, et al. 2020. Functional annotation of rare structural variation in the human brain. *Nature Communications* **11**. <http://dx.doi.org/10.1038/s41467-020-16736-1>.

Hormozdiari F, Kostem E, Kang EY, Pasaniuc B, Eskin E. 2014. Identifying Causal Variants at Loci with Multiple Signals of Association. *Genetics* **198**: 497–508.

Hormozdiari F, van de Bunt M, Segre AV, Li X, Joo JWJ, Bilow M, Sul JH, Sankararaman S, Pasaniuc B, Eskin E. 2016. Colocalization of GWAS and eQTL Signals Detects Target Genes. *Am J Hum Genet* **99**: 1245–1260.

International Schizophrenia Consortium. 2008. Rare chromosomal deletions and duplications increase risk of schizophrenia. *Nature* **455**: 237–241.

Jakubosky D, D'Antonio M, Bonder MJ, Smail C, Donovan MKR, Young Greenwald WW, Matsui H, i2QTL Consortium, D'Antonio-Chronowska A, Stegle O, et al. 2020. Properties of structural variants and short tandem repeats associated with gene expression and complex traits. *Nat Commun* **11**: 2927.

Kent WJ, Sugnet CW, Furey TS, Roskin KM, Pringle TH, Zahler AM, Haussler D. 2002. The human genome browser at UCSC. *Genome Res* **12**: 996–1006.

Kundaje A, Meuleman W, Ernst J, Bilenky M, Yen A, Heravi-Moussavi A, Kheradpour P, Zhang Z, Wang J, Ziller MJ, et al. 2015. Integrative analysis of 111 reference human epigenomes. *Nature* **518**: 317–330.

Lappalainen T, Sammeth M, Friedlander MR, t Hoen PA, Monlong J, Rivas MA, Gonzalez-Porta M, Kurbatova N, Griebel T, Ferreira PG, et al. 2013. Transcriptome and genome sequencing uncovers functional variation in humans. *Nature* **501**: 506–511.

Larson DE, Abel HJ, Chiang C, Badve A, Das I, Eldred JM, Layer RM, Hall IM. 2019. svtools: population-scale analysis of structural variation. *Bioinformatics* **35**: 4782–4787.

Layer RM, Chiang C, Quinlan AR, Hall IM. 2014. LUMPY: a probabilistic framework for structural variant discovery. *Genome Biol* **15**: R84.

Li X, Kim Y, Tsang EK, Davis JR, Damani FN, Chiang C, Hess GT, Zappala Z, Strober BJ, Scott AJ, et al. 2017. The impact of rare variation on gene expression across tissues. *Nature* **550**: 239–243.

Marshall CR, Howrigan DP, Merico D, Thiruvahindrapuram B, Wu W, Greer DS, Antaki D, Shetty A, Holmans PA, Pinto D, et al. 2017. Contribution of copy number variants to schizophrenia from a genome-wide study of 41,321 subjects. *Nat Genet* **49**: 27–35.

McCarthy SE, Makarov V, Kirov G, Addington AM, McClellan J, Yoon S, Perkins DO, Dickel DE, Kusenda M, Krastoshevsky O, et al. 2009. Microduplications of 16p11.2 are associated with schizophrenia. *Nat Genet* **41**: 1223–1227.

McKenna A, Hanna M, Banks E, Sivachenko A, Cibulskis K, Kernytsky A, Garimella K, Altshuler D, Gabriel S, Daly M, et al. 2010. The Genome Analysis Toolkit: a MapReduce framework for analyzing next-generation DNA sequencing data. *Genome Res* **20**: 1297–1303.

Ongen H, Buil A, Brown AA, Dermitzakis ET, Delaneau O. 2016. Fast and efficient QTL mapper for thousands of molecular phenotypes. *Bioinformatics* **32**: 1479–1485.

Payer LM, Burns KH. 2019. Transposable elements in human genetic disease. *Nat Rev Genet* **20**: 760–772.

Quinlan AR, Hall IM. 2010. BEDTools: a flexible suite of utilities for comparing genomic features. *Bioinformatics* **26**: 841–842.

Sebat J, Lakshmi B, Malhotra D, Troge J, Lese-Martin C, Walsh T, Yamrom B, Yoon S, Krasnitz A, Kendall J, et al. 2007. Strong association of de novo copy number mutations with autism. *Science* **316**: 445–449.

Stranger BE, Forrest MS, Dunning M, Ingle CE, Beazley C, Thorne N, Redon R, Bird CP, de Grassi A, Lee C, et al. 2007. Relative impact of nucleotide and copy number variation on gene expression phenotypes. *Science* **315**: 848–853.

Sudmant PH, Rausch T, Gardner EJ, Handsaker RE, Abyzov A, Huddleston J, Zhang Y, Ye K, Jun G, Hsi-Yang Fritz M, et al. 2015. An integrated map of structural variation in 2,504 human genomes. *Nature* **526**: 75–81.

Turner TN, Coe BP, Dickel DE, Hoekzema K, Nelson BJ, Zody MC, Kronenberg ZN, Hormozdiari F, Raja A, Pennacchio LA, et al. 2017. Genomic Patterns of De Novo Mutation in Simplex Autism. *Cell* **171**: 710–722.e12.

Turner TN, Eichler EE. 2019. The Role of De Novo Noncoding Regulatory Mutations in Neurodevelopmental Disorders. *Trends Neurosci* **42**: 115–127.

Walsh T, McClellan JM, McCarthy SE, Addington AM, Pierce SB, Cooper GM, Nord AS, Kusenda M, Malhotra D, Bhandari A, et al. 2008. Rare Structural Variants Disrupt Multiple Genes in Neurodevelopmental Pathways in Schizophrenia. *Science* **320**: 539–543.
<http://dx.doi.org/10.1126/science.1155174>.

Weiss LA, Shen Y, Korn JM, Arking DE, Miller DT, Fossdal R, Saemundsen E, Stefansson H, Ferreira MA, Green T, et al. 2008. Association between microdeletion and microduplication at 16p11.2 and autism. *N Engl J Med* **358**: 667–675.

Yang J, Lee SH, Goddard ME, Visscher PM. 2011. GCTA: a tool for genome-wide complex trait analysis. *Am J Hum Genet* **88**: 76–82.

Zhao H, Sun Z, Wang J, Huang H, Kocher J-P, Wang L. 2014. CrossMap: a versatile tool for coordinate conversion between genome assemblies. *Bioinformatics* **30**: 1006–1007.

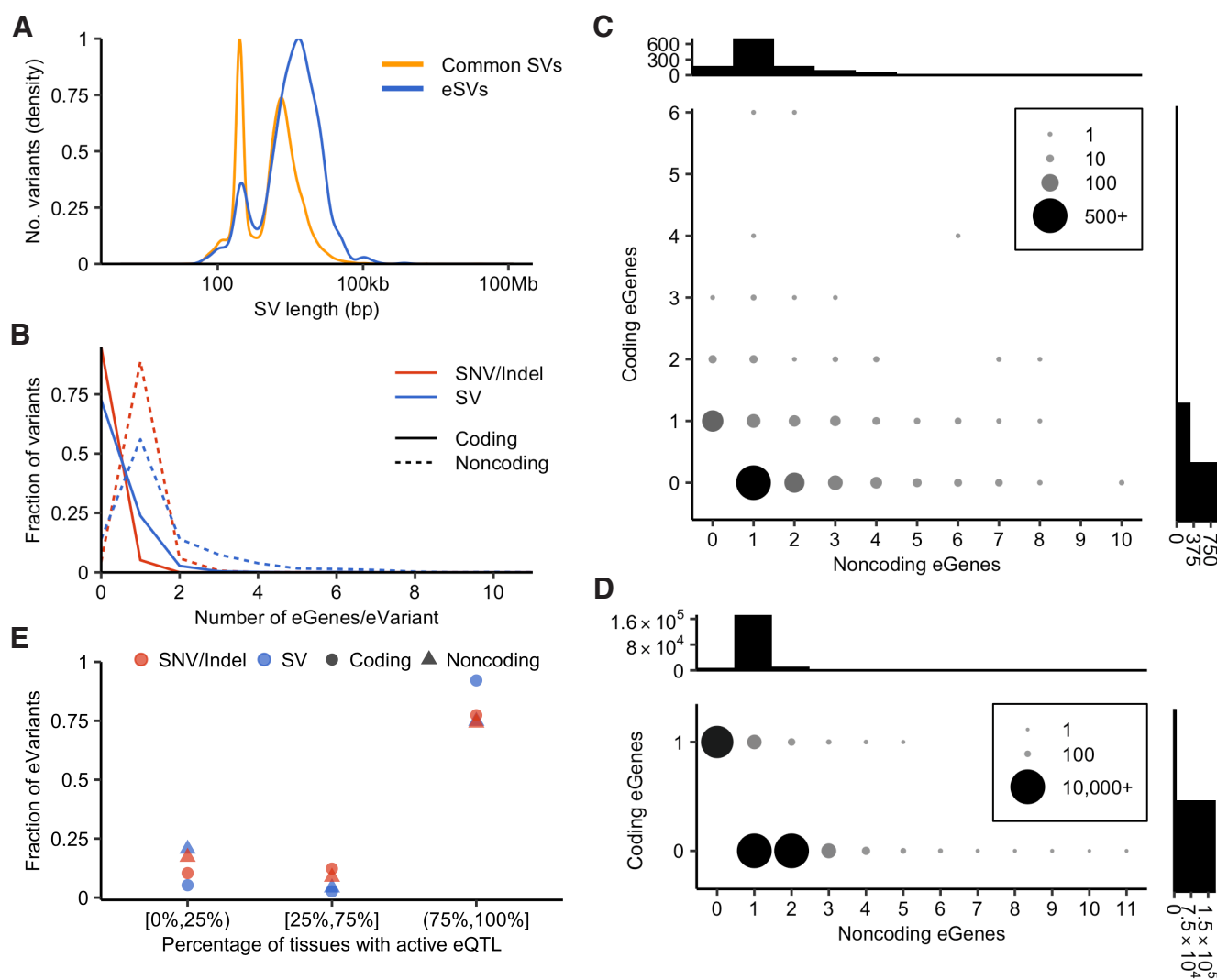


Figure 1. Features of SV-eQTLs. (A) Size distribution of eSVs compared to all common SVs. (B) Distribution of the number of eGenes per eVariant for SVs compared to SNVs and indels. “Coding” eGenes refer to eGenes whose exons are intersected by the associated eVariant and “noncoding” eGenes are not intersected by the associated eVariant. Counts are shown for every eVariant, thus eVariants with zero coding or zero noncoding eGenes are included in the distributions. (C,D) The number of eVariants, as shown by dot size and color, with the indicated combination of coding and noncoding eGenes, as defined above. Shown for SVs (C) and SNV/indels (D), with histograms showing the total number of eVariants with the indicated number of associated coding or noncoding eGenes above the y- and x-axes, respectively. (E) Distribution of tissue specificity of eQTLs across tissues as evaluated by METASOFT, separated into the lowest quartile, middle two quartiles and top quartile, for eQTLs in which the activity status is known in at least 43 of 48 evaluated tissues. The points indicate the fraction of SV-eQTLs or SNV- and indel-eQTLs that are active ($m > 0.9$) in the proportion of tissues indicated on the x-axis.

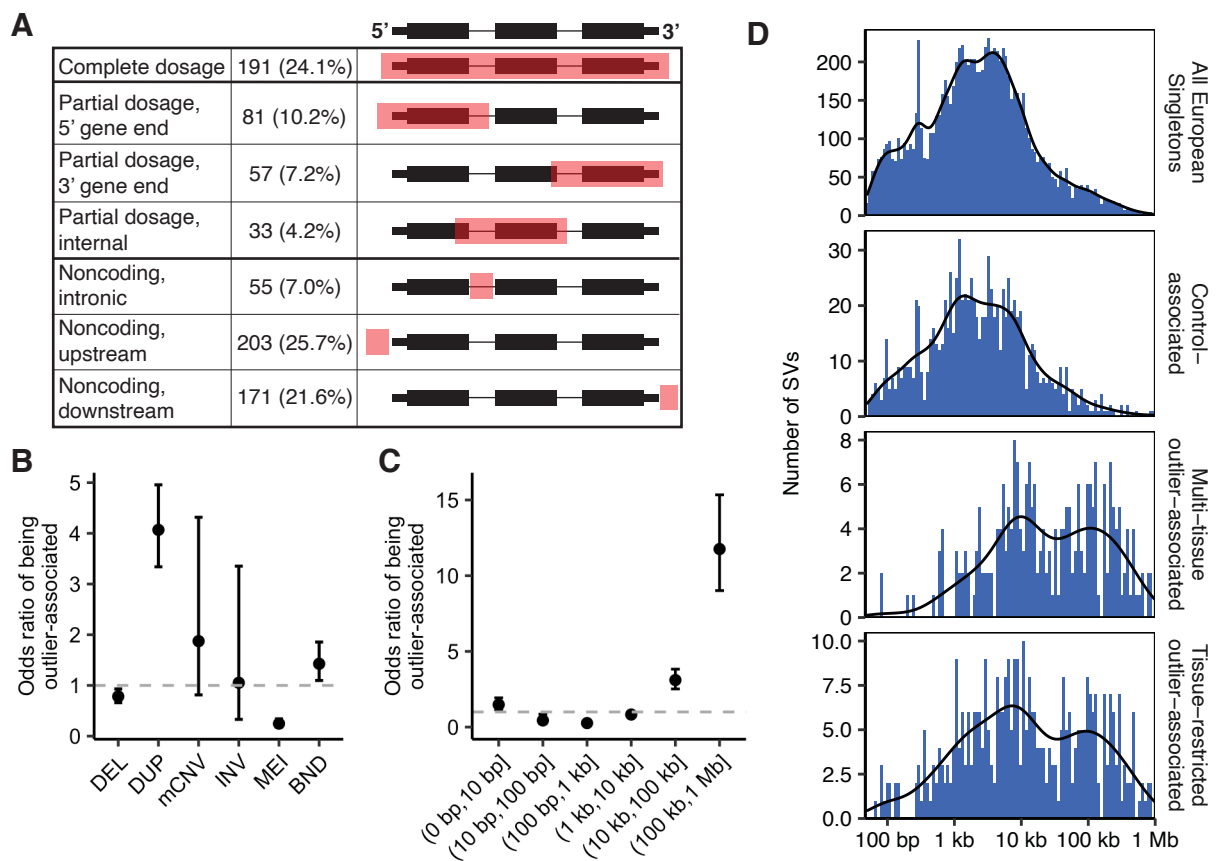


Figure 2. Features of outliner-associated SVs. (A) Location of outliner-associated SVs relative to their associated outlier gene and the number of SV/outlier gene associations identified in each category. Percentages indicate the fraction of outliner/SV pairs found at each relative location compared to the total number of SV/outlier gene associations. Note that this definition allows one SV to be associated with multiple outlier genes and thus the SV is counted in multiple categories. Gene diagrams provide examples of possible SV location, shown in red, relative to the outlier gene. (B,C) Odds ratio (OR) of being outliner-associated by SV type (B) and SV size (C) for the SV category of interest compared to all other SVs. Note that BNDs were excluded from the size OR calculations due to their ambiguous nature and thus size. (D) Distribution of SV sizes for singleton SVs smaller than 1 Mb identified in European individuals that were used in outliner analyses. Panels depict size distributions for all European-cohort singlettons, control-associated singlettons, multi-tissue outliner-associated singlettons and tissue-restricted outliner-associated singlettons.

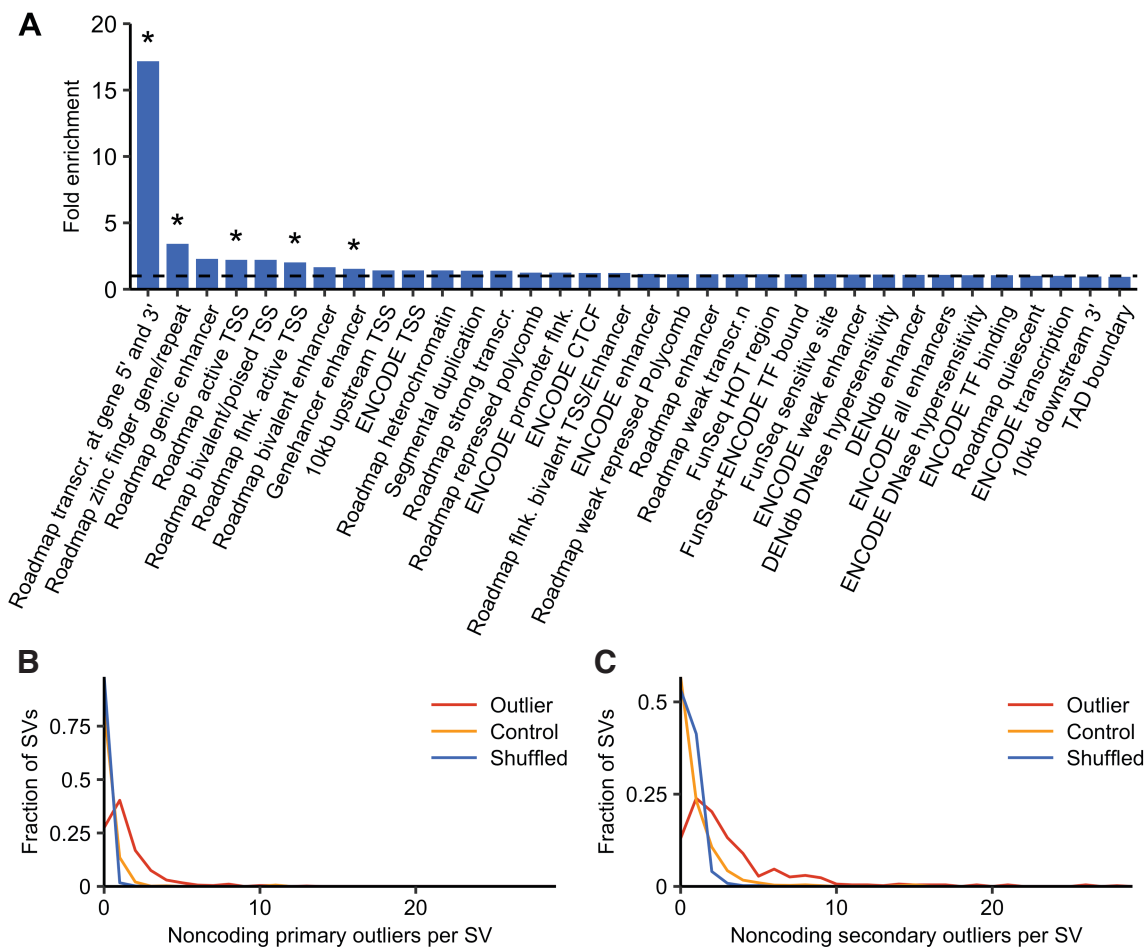


Figure 3. Mechanistic insights into outlier-associated SVs. (A) Enrichment of outlier-associated SVs in functional genomic annotations compared to control-associated SVs. Asterisks indicate statistical significance based on a Fisher's exact test with Bonferroni correction for multiple testing. **(B,C)** The distribution of the number of noncoding primary (B) and secondary (C) outliers found within 1 Mb of the region surrounding tissue-restricted outlier-associated SVs, control-associated SVs and a shuffled null.